

# Effect of Fermi surface shape on transport properties in $Fe_{1-x}Ni_xTiSb$ half-Heusler alloys.

T.Stopa, J. Tobiła and S.Kaprzyk  
 Faculty of Physics and Applied Computer Science,  
 AGH University of Science and Technology, 30-059 Kraków, Poland  
 (Dated: 16 September 2004)

We report results of conductivity and Seebeck coefficient calculations for  $Fe_{1-x}Fe_xTiSb$  half-Heusler alloys with various  $x$  contents. As a computational method we use the Korringa-Kohn-Rostoker (KKR) formalism with coherent potential approximation (CPA). Our main goal was to determine the Fermi surface topology changes with  $Ni$  alloying. Because the geometry of Fermi surface affects the conductivity and Seebeck coefficient, we were able to elucidate the main mechanism responsible for the experimentally observed transport features. When passing through the concentration  $x = 0.5$ , the Fermi surface change from the electronic-like to the hole-like form, which clearly explains the sign changing in Seebeck coefficient.

## I. INTRODUCTION

$Fe_{1-x}Ni_xTiSb$  compound exhibits very interesting transport properties which were both measured experimentally and predicted theoretically[1]. It crystallizes in half-Heusler structure, which consists of three fcc sublattices displayed along the diagonal of the unit cell:  $(0, 0, 0)$ ,  $(\frac{1}{4}, \frac{1}{4}, \frac{1}{4})$  and  $(\frac{3}{4}, \frac{3}{4}, \frac{3}{4})$ , as shown in Fig.1. For small  $Ni$  content the alloy exhibits metallic properties and was found to be a Curie-Weiss paramagnet. For  $x \approx 0.5$  it's character changes to semiconducting one, while for  $x \approx 1.0$  changes again to metallic, but this time as Pauli paramagnet.

Measurements of Seebeck coefficient at 300 K are bringing very interesting results. It's small value at  $x = 0.25$  grows reaching maximum at  $x = 0.4$ , and falls down almost to zero near  $x = 0.5$ . Then changes sign passing through minimum and at  $x = 0.75$  approaching back the almost zero value.

In the present work use a modified computational

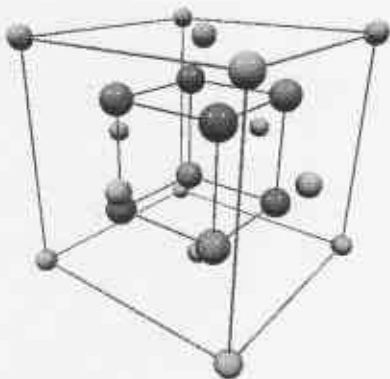


FIG. 1: Crystal structure of the half-Heusler  $Fe_{1-x}Ni_xTiSb$  compound. The Fe(Ni) atoms are shown green, Ti atoms are blue and Sb atoms are red.

technique based on the Korringa-Kohn-Rostoker (KKR) formalism[2][3] with coherent potential approximation (CPA)[4][5][6] for calculating electronic properties of disordered systems. With this technique applied to  $Fe_{1-x}Ni_xTiSb$  system for  $x = 0.25, 0.4, 0.5, 0.6$  and  $0.75$  we computed conductivity with energy dependence and subsequently Seebeck coefficients without any adjustable parameters. A reasonably good agreement with experimental results gives us confidence that KKR-CPA theory is adequate enough to study thermoelectric properties of alloys.

## II. COMPUTATIONAL METHOD

In this work we focused on calculating conductivity and Seebeck coefficients which are given by the following formulas[7][8]:

$$\sigma(E) = \frac{2e^2}{3(2\pi)^3\hbar} \int_{\Sigma(E)} dS_{\mathbf{k}} v_{\mathbf{k}} \tau_{\mathbf{k}} \quad (1)$$

$$S = -\frac{\pi^2 k_B^2 T}{3e} \left. \frac{\partial \ln \sigma(E)}{\partial E} \right|_{E_F} \quad (2)$$

where  $S$  is Seebeck coefficient,  $\sigma(E_F)$  is conductivity,  $v_{\mathbf{k}}$  and  $\tau_{\mathbf{k}}$  stand for the group velocity and life-time of electron with  $\mathbf{k}$ -vector on constant energy surface  $\Sigma(E)$ . In practical computations we use the self-consistent KKR-CPA code, which allows energy to be complex. After selfconsistency on electronic charges and effective potential was achieved, we computed electronic bands with complex energy values and then numerically determined group velocities of electrons from real part of  $E(\mathbf{k})$ :

$$\mathbf{v}_{\mathbf{k}} = \frac{1}{\hbar} \nabla_{\mathbf{k}} [ReE(\mathbf{k})] \quad (3)$$

and life-times from imaginary part  $ImE(\mathbf{k})$ :

$$\tau_{\mathbf{k}} = \frac{\hbar}{ImE(\mathbf{k})} \quad (4)$$

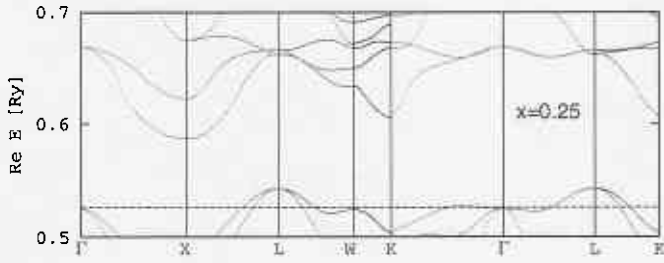


FIG. 2: Energy bands in  $Fe_{1-x}Ni_xTiSb$  for  $x = 0.25$ .

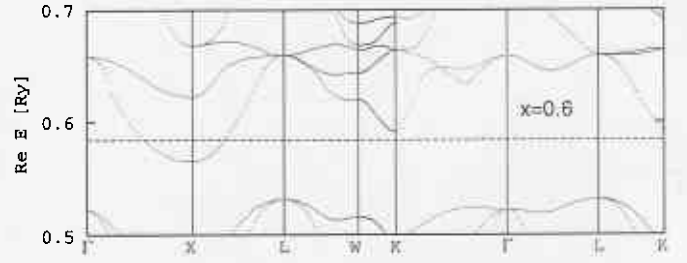


FIG. 5: Energy bands in  $Fe_{1-x}Ni_xTiSb$  for  $x = 0.6$ .

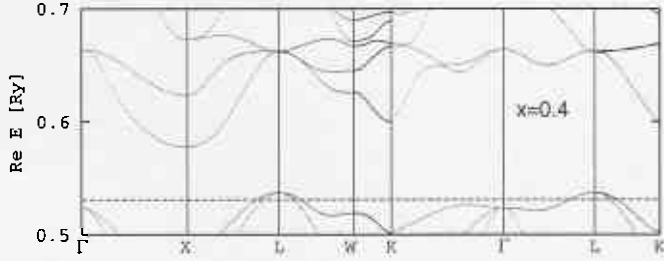


FIG. 3: Energy bands in  $Fe_{1-x}Ni_xTiSb$  for  $x = 0.4$ .

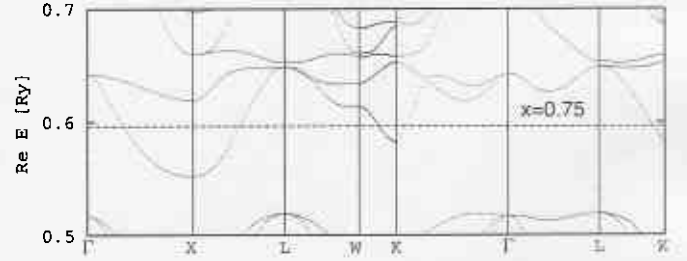


FIG. 6: Energy bands in  $Fe_{1-x}Ni_xTiSb$  for  $x = 0.75$ .

### III. BAND STRUCTURE AND FERMI SURFACES

The KKR-CPA mentioned in the previous section we applied to  $Fe_{1-x}Ni_xTiSb$  system with  $x = 0.25, 0.4, 0.5, 0.6$  and  $0.75$ . Resulting energy bands, along high symmetry lines, and energy window near  $E_F$  are plotted in Fig.2 - Fig.6, for each of the Ni concentrations respectively. Only real part of energy bands is shown here. One can see, that the system with  $x = 0.25$  and  $x = 0.4$  is metallic with two bands crossing  $E_F$ , and hole-like behavior. For the concentration  $x = 0.5$  the Fermi energy falls into the middle of energy gap. The system becomes semiconducting (Fermi surface vanishes) and according to (1) and (2) both conductivity and Seebeck coefficient are zero. Finally, for the  $x = 0.6$  and  $x = 0.75$ , one band crosses Fermi energy and alloy becomes metallic again but this time with electronic-like behavior. Fermi surfaces, generated numerically from the bands on the dense mesh of  $k$ -points, are shown in

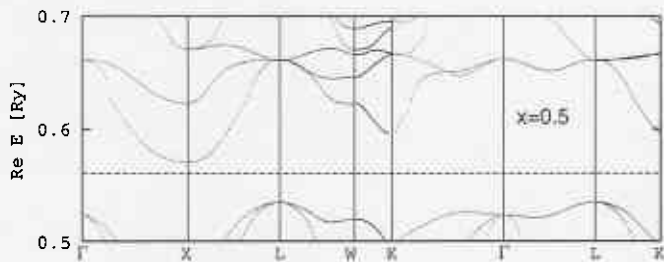


FIG. 4: Energy bands in  $Fe_{1-x}Ni_xTiSb$  for  $x = 0.5$  (semiconductor).

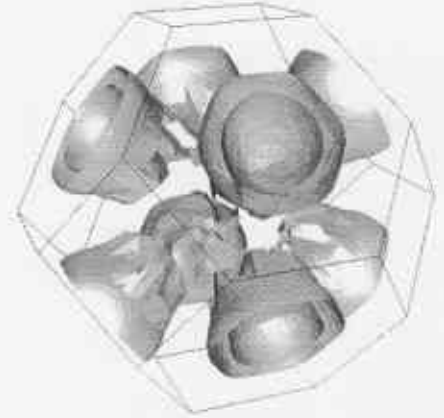


FIG. 7: Fermi surface of  $Fe_{0.75}Ni_{0.25}TiSb$  ( $x = 0.25$ ).

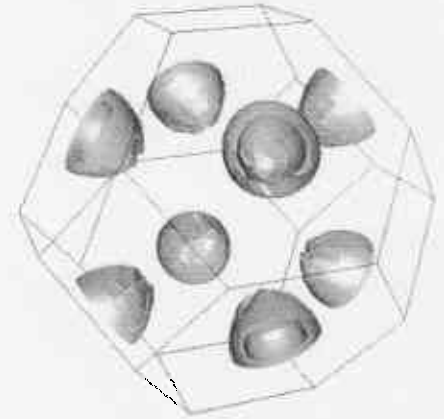


FIG. 8: Fermi surface of  $Fe_{0.6}Ni_{0.4}TiSb$  ( $x = 0.4$ ).

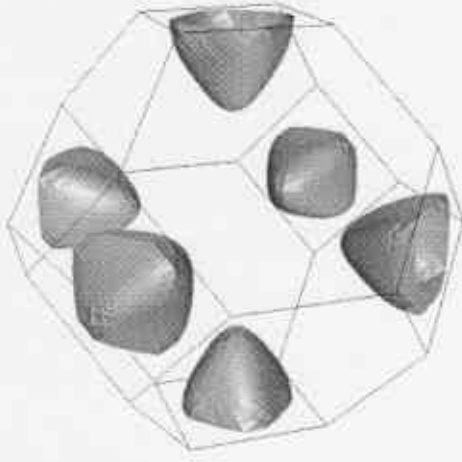


FIG. 9: Fermi surface of  $Fe_{0.4}Ni_{0.6}TiSb$  ( $x = 0.6$ ).

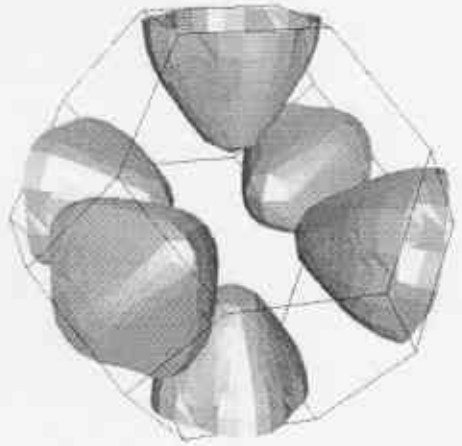


FIG. 10: Fermi surface of  $Fe_{0.25}Ni_{0.75}TiSb$  ( $x = 0.75$ ). In this figure for clarity we did not apply periodic boundary conditions, so the Fermi surface goes out of the Brillouin zone, but it's better visible.

Fig.7 and Fig.8 for  $x = 0.25$  and  $x = 0.4$ , with the two-sheets appearance due to two bands crossing  $E_F$  in these cases. Similarly, in Fig.9 and Fig.10, we show one-sheet Fermi surfaces for  $x = 0.6$  and  $x = 0.75$ . One can imagine, that they have a finite thickness which results from the nonzero imaginary part of energy. For  $x < 0.5$ , two Fermi sheets are centered in the middle of the hexagonal walls of the Brillouin zone. If generating constant energy surface for the energy little above  $E_F$  for these cases, the cups get smaller, reflecting it's hole-like form, with electrons outside the cups. For  $x > 0.5$ , single-sheet Fermi surface cups are centered in the middles of the square walls of the Brillouin zone. Contrary to the previous case ( $x < 0.5$ ) with increasing energy the volume of the cups grows, reflecting it's electron-like form, with electrons inside of the cups. The observed geometry of Fermi surface changes then, when crossing  $x = 0.5$ , from hole-like to electron-like and is responsible for Seebeck

$x$	$\rho_{calc}^{0K} (\mu\Omega m)$	$\rho_{exp}^{300K} (\mu\Omega m)$
0.25	0.15	4.1
0.4	0.64	19.1
0.5	$\infty$	134.7
0.6	1.13	90.8
0.75	0.31	4.2

TABLE I: Calculated and measured[1] conductivities in  $Fe_{1-x}Ni_xTiSb$ . Experimental values were taken in room-temperature while calculated ones describe the ground state.

$x$	$S/T (\mu V/K^2)$	$S/T \cdot 300K (\mu V/K)$	$S_{exp}^{300K} (\mu V/K)$
0.25	-0.04	-12	$\approx 0$
0.4	0.4	120	124
0.5	0	0	33
0.6	-0.13	-39	-112
0.75	-0.05	-15	$\approx 0$

TABLE II: Calculated and measured[1] Seebeck coefficients in  $Fe_{1-x}Ni_xTiSb$ . Experimental values are at 300K. Calculated  $S/T$  values were multiplied by 300K since the temperature dependence of  $S$  is linear as can be seen in (1).

coefficient sign changing.

#### IV. TRANSPORT PROPERTIES

After generating and setting numerical data bases for Fermi surfaces for various Ni concentrations, we used equations (1) and (2) to calculate energy dependent conductivities and Seebeck coefficients. The obtained results are collected and shown in Table 1 and Table 2. As the calculations were done for the ground state of the system, it means that the life-time of electrons is only due to atomic disorder (Fe, or Ni) on one of sublattices. In higher temperature also the disorder due to thermal vibrations of atoms (phonons) have to be included, what is not done here. This kind of disorder becomes essential for crystalline materials, and must be used if computing Seebeck coefficients for FeTiSb or NiTiSb compounds. If all those factors, which are present in the experimental results, would be included into our calculations, we expect further improvement in agreement between theory and experiment curves shown in Fig. 11.

#### V. CONCLUSIONS

We presented the first principle calculations of the transport properties of alloys, using KKR-CPA theory. Applying it to the  $Fe_{1-x}Ni_xTiSb$  system ( $x = 0.25, 0.4, 0.5, 0.6$  and  $0.75$ ), from the complex energy bands on dense mesh of  $k$ -points in Brillouin zone, we generated Fermi surfaces and then calculated conductivity with energy dependence and subsequently Seebeck

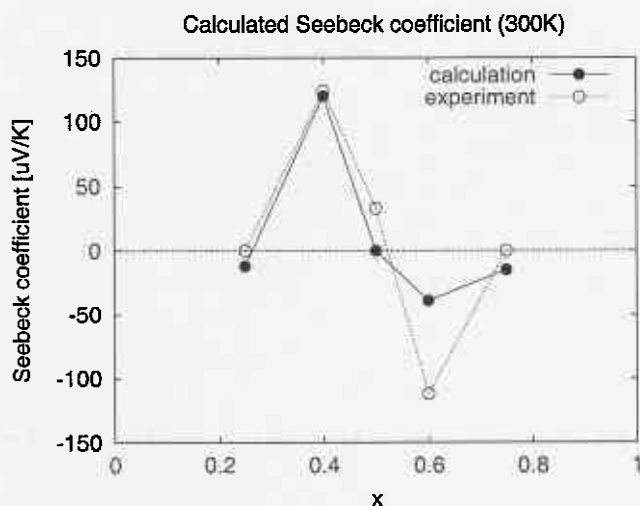


FIG. 11: Calculated and measured[1] Seebeck coefficients for various Ni contents.

coefficients. Although our results do not include lattice thermal vibrations, they agree quite well with the experimental data at room temperature (under assumption of linear temperature dependence of  $S$ ). In particular, we clearly show the composition-induced metal-semiconductor-metal transition. It would be very interesting to compare the present results with the low-temperature measurements.

- [1] J.Tobola, L.Jodin, P.Peucher and H.Scherrer, *Phys. Rev. B* **64**, 155103 (2001)  
 [2] J.Korringa, *Physica* **13**, 392 (1947)  
 [3] W.Kohn and N.Rostoker, *Phys. Rev.* **94**, 1111 (1954)  
 [4] P.Soven, *Phys. Rev.* **156**, 809 (1967)  
 [5] A.Bansil, S.Kaprzyk, P.E.Mijnarends and J.Tobola, *Phys. Rev. B* **60**, 13396 (1999)

- [6] S.Kaprzyk and A.Bansil, *Phys. Rev. B* **26**, 367 (1982)  
 [7] W.H.Butler and G.M.Stocks, *Phys. Rev. B* **29**, 4217 (1984)  
 [8] N.W. Ashcroft and N.D. Mermin, *Solid State Physics*, (1976)